32nd URSI GASS, Montreal, 19–26 August 2017

High Frequency Plane Wave Scattering Analysis from Dielectric Cuboids – TM Polarization –

Hieu Ngoc Quang (1), Hiroshi Shirai (1)
(1) Chuo University, Tokyo, Japan

Abstract

Scattering field from a dielectric cuboid illuminated by a transverse magnetic (TM) polarized plane wave is formulated by Kirchhoff approximation. First, the equivalent currents have been derived for the forward scattering field by the reflected electric and magnetic fields, then the scattering far fields are generated by the postulated equivalent currents flowing on the surfaces. Effects of multiple internal bouncing caused by the finiteness of dielectric scattering body are included. A good agreement between theoretical estimation and HFSS simulation has been shown.

1 Introduction

Dielectric materials can be electrically parameterized by their dielectric constants, and these values as well as their dimensions are important for identifying the scattering objects. Electromagnetic scattering studies of dielectric materials have gained increasing importance in the research fields, such as radar applications, anti-radar designs, etc.

In electromagnetic wave scattering study, high frequency asymptotic methods have been used widely to obtain approximate solutions. Among these approaches, Kirchhoff approximation is a powerful and comprehensive method [1]. As a part of this approximation method, the conventional Physical Optics (PO) method postulates to calculate the scattering far-field generated by the electric current on the perfectly conducting surface [2, 3]. However, the conventional PO method cannot be implemented on dielectric bodies.

In this study, the main objective is to formulate a general three-dimensional (3D) scattering field from dielectric cuboids using Kirchhoff approximation. The scattering fields are generated by the postulated electric and magnetic equivalent currents excited by the reflected electric and magnetic fields. The comparable scattering problem due to the complementary transverse electric (TE) polarization case has already been formulated for dielectric cylinders [4] and dielectric cuboids [5]. In this presentation, the scattering by a transverse magnetic (TM) polarized plane wave is investigated. The Radar Cross Section (RCS) is derived to compare with other methods.

2 Formulations

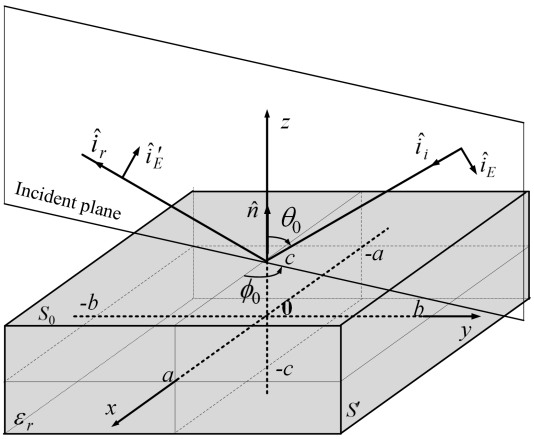

Figure 1. Scattering from a dielectric cuboid.

Let us consider an oblique incidence of a transverse magnetic polarized plane wave on a dielectric cuboid, whose cross sectional surface S_0 is $2a \times 2b$, its depth is $2c$, and the relative permittivity is ε_r, as shown in Fig. 1. The incident TM plane wave has the following form:

$$\begin{aligned} \boldsymbol{E}^i &= E_0(\cos\theta_0\cos\phi_0\hat{\boldsymbol{x}} + \cos\theta_0\sin\phi_0\hat{\boldsymbol{y}} - \sin\theta_0\hat{\boldsymbol{z}}) \\ &\quad e^{ik(-x\sin\theta_0\cos\phi_0 - y\sin\theta_0\sin\phi_0 - z\cos\theta_0)}, \end{aligned} \tag{1}$$

$$\begin{aligned} \boldsymbol{H}^i &= \frac{E_0}{Z_0}(\sin\phi_0\hat{\boldsymbol{x}} - \cos\phi_0\hat{\boldsymbol{y}}) \\ &\quad e^{ik(-x\sin\theta_0\cos\phi_0 - y\sin\theta_0\sin\phi_0 - z\cos\theta_0)}, \end{aligned} \tag{2}$$

where k, Z_0 denote the wave number, wave impedance in free space, respectively. Then, the reflected wave from the top surface of the cuboid may be written as

$$\begin{aligned} \boldsymbol{E}^r &= \Gamma_m(\theta_0)E_0(\cos\theta_0\cos\phi_0\hat{\boldsymbol{x}} + \cos\theta_0\sin\phi_0\hat{\boldsymbol{y}} + \sin\theta_0\hat{\boldsymbol{z}}) \\ &\quad e^{ik[-x\sin\theta_0\cos\phi_0 - y\sin\theta_0\sin\phi_0 - (2c-z)\cos\theta_0]}, \end{aligned} \tag{3}$$

$$\begin{aligned} \boldsymbol{H}^r &= \frac{\Gamma_m(\theta_0)E_0}{Z_0}(-\sin\phi_0\hat{\boldsymbol{x}} + \cos\phi_0\hat{\boldsymbol{y}}) \\ &\quad e^{ik[-x\sin\theta_0\cos\phi_0 - y\sin\theta_0\sin\phi_0 - (2c-z)\cos\theta_0]}. \end{aligned} \tag{4}$$

Here $\Gamma_m(\theta_0)$ represents the collective reflection coefficient when one considers a finite thickness and the multiple bouncing effect of scattering dielectric body, and is given by

$$\Gamma_m(\theta_0) = \frac{\Gamma_s(\theta_0)(1 - e^{i4kc\sqrt{\varepsilon_r - \sin^2\theta_0}})}{1 - \Gamma_s^2(\theta_0)e^{i4kc\sqrt{\varepsilon_r - \sin^2\theta_0}}}, \tag{5}$$

with $\Gamma_s(\theta_0)$ is a conventional reflection coefficient from the surface S_0,

$$\Gamma_s(\theta_0) = -\frac{\varepsilon_r \cos\theta_0 - \sqrt{\varepsilon_r - \sin^2\theta_0}}{\varepsilon_r \cos\theta_0 + \sqrt{\varepsilon_r - \sin^2\theta_0}}. \quad (6)$$

Accordingly, equivalent electric and magnetic currents on the top surface S_0 of the cuboid ($-a \le x \le a$, $-b \le y \le b$, $z = c$) may be derived from the reflected field by $\boldsymbol{J} = \hat{\boldsymbol{n}} \times \boldsymbol{H}^r$, $\boldsymbol{M} = \boldsymbol{E}^r \times \hat{\boldsymbol{n}}$ as

$$\begin{aligned} \boldsymbol{J}(x,y) &= \frac{\Gamma_m(\theta_0)E_0}{Z_0}(-\cos\phi_0\hat{\boldsymbol{x}} - \sin\phi_0\hat{\boldsymbol{y}}) \\ &\quad e^{ik(-x\sin\theta_0\cos\phi_0 - y\sin\theta_0\sin\phi_0 - c\cos\theta_0)}, \quad (7) \\ \boldsymbol{M}(x,y) &= \Gamma_m(\theta_0)E_0(\cos\theta_0\sin\phi_0\hat{\boldsymbol{x}} - \cos\theta_0\cos\phi_0\hat{\boldsymbol{y}}) \\ &\quad e^{ik(-x\sin\theta_0\cos\phi_0 - y\sin\theta_0\sin\phi_0 - c\cos\theta_0)}. \quad (8) \end{aligned}$$

Then the radiation field due to these currents $\boldsymbol{J}$ and $\boldsymbol{M}$ on S_0 may be calculated using electric and magnetic vector potentials $\boldsymbol{A}$ and $\boldsymbol{F}$:

$$\boldsymbol{A} = \frac{\mu_0}{4\pi}\int_{S_0} \boldsymbol{J}(\boldsymbol{r}')\frac{e^{ik|\boldsymbol{r}-\boldsymbol{r}'|}}{|\boldsymbol{r}-\boldsymbol{r}'|}dS', \quad (9)$$

$$\boldsymbol{F} = \frac{\varepsilon_0}{4\pi}\int_{S_0} \boldsymbol{M}(\boldsymbol{r}')\frac{e^{ik|\boldsymbol{r}-\boldsymbol{r}'|}}{|\boldsymbol{r}-\boldsymbol{r}'|}dS', \quad (10)$$

where $\boldsymbol{r}$, $\boldsymbol{r}'$ denote the position vectors to the observation and current source points, respectively. Assuming that the observation is far from the cuboid, one can use the far field approximation to evaluate the above integrals analytically. Thus, the total scattering field in the spherical coordinate system (r, θ, ϕ) may be expressed as

$$\begin{aligned} E_r^s &= 0, \quad (11) \\ E_\theta^s &= -\frac{i}{k\pi}\Gamma_m(\theta_0)E_0\frac{e^{ikr}}{r}e^{-ikc(\cos\theta+\cos\theta_0)} \\ &\quad (\cos\theta + \cos\theta_0)\cos(\phi - \phi_0)F, \quad (12) \\ E_\phi^s &= \frac{i}{k\pi}\Gamma_m(\theta_0)E_0\frac{e^{ikr}}{r}e^{-ikc(\cos\theta+\cos\theta_0)} \\ &\quad (1 + \cos\theta_0\cos\theta)\sin(\phi - \phi_0)F, \quad (13) \end{aligned}$$

where

$$F = \frac{\sin[ka(\sin\theta\cos\phi + \sin\theta_0\cos\phi_0)]}{\sin\theta\cos\phi + \sin\theta_0\cos\phi_0} \cdot \frac{\sin[kb(\sin\theta\sin\phi + \sin\theta_0\sin\phi_0)]}{\sin\theta\sin\phi + \sin\theta_0\sin\phi_0}. \quad (14)$$

Then, the radar cross sections (RCS) are given by

$$\begin{aligned} \sigma_{\theta\theta} &= \lim_{r\to\infty} 4\pi r^2 \frac{|\boldsymbol{E}_\theta^s|^2}{|\boldsymbol{E}^i|^2} \\ &= \frac{4|\Gamma_m(\theta_0)|^2F^2}{\pi k^2}(\cos\theta + \cos\theta_0)^2\cos^2(\phi - \phi_0), \quad (15) \\ \sigma_{\phi\theta} &= \lim_{r\to\infty} 4\pi r^2 \frac{|\boldsymbol{E}_\phi^s|^2}{|\boldsymbol{E}^i|^2} \\ &= \frac{4|\Gamma_m(\theta_0)|^2F^2}{\pi k^2}(\cos\theta\cos\theta_0 + 1)^2\sin^2(\phi - \phi_0). \quad (16) \end{aligned}$$

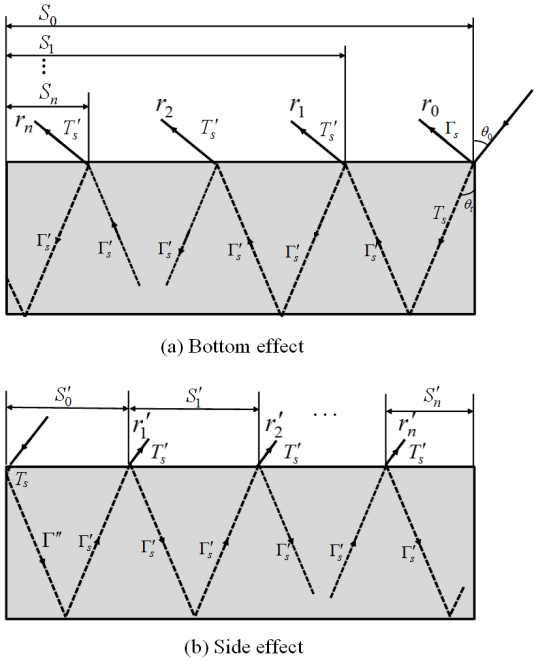

Figure 2. Multiple bouncing effect.

3 Numerical Results and Discussion

The electromagnetic scattering from a dielectric cuboid is more complex since the incident wave penetrates inside the cuboid body and excites the internal reflected and transmitted wave as shown in Fig. 2. When the incident plane wave impinges on a cuboid, the specular reflection $\Gamma_s(\theta_0)$ and transmission $T_s(\theta_0)$ occurs at the top surface S_0, where the equivalent currents $\boldsymbol{J}_0$, $\boldsymbol{M}_0$ will be excited. As the internal reflection $\Gamma'_s(\theta_0)$ and the transmission $T_s'(\theta_0)$ continue, the additional equivalent currents $\boldsymbol{J}_n$, $\boldsymbol{M}_n$ will flow on the range S_n of the finally departing rays r_n.

Because of the finite lateral length, the internal bouncing rays r_n will be terminated. Accordingly the collective reflection coefficient $\Gamma_m(\theta_0)$ is only correct for the normal incident ($\theta_0 = 0$). When the internal bouncing rays reflect at the side surface at $y = \pm b$, and emit the transmitted rays r_n'. The additional rays excite the equivalent currents $\boldsymbol{J}_n'$, $\boldsymbol{M}_n'$ flowing on range S_n'. The scattering field formulation due to the internal bouncing rays is similar with (11)–(13), but with different currents and ranges.

In order to validate our approximation, monostatic RCS has been calculate and compare with other results [6]. The investigated objects are dielectric cuboids of the permittivity $\varepsilon_r = 6.40 + i0.11$ (Material 1) and $\varepsilon_r = 3.40 + i0.25$ (Material 2). The analytical monostatic RCS $\sigma_{\theta\theta}$ from the top surface of the cuboids of Material 1 is shown in Fig. 3. Here the dimension of the cuboid is 100 mm $\times$ 100 mm $\times$ 100 mm and the frequency is 24 GHz. The results are compared with the those by surface reflection only and internal bouncing effect from the bottom. One observes an internal bouncing effect even at specular reflection direction, and

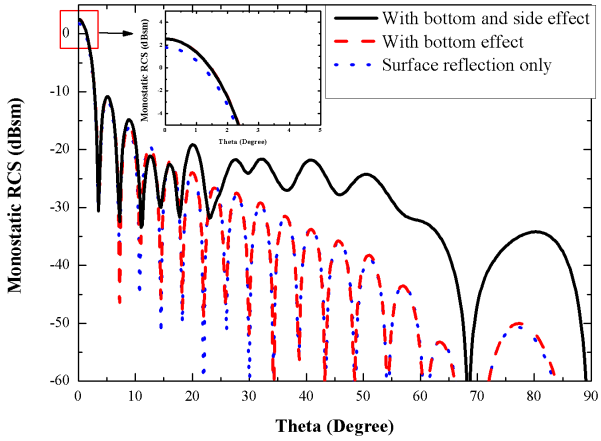

Figure 3. Monostatic RCS $\sigma_{\theta\theta}$ at 24 GHz from the top surface of a cuboid. $a = b = c = 50$ mm, $\varepsilon_r = 6.40 + i0.11$ and $\phi = \phi_0 = 90^o$.

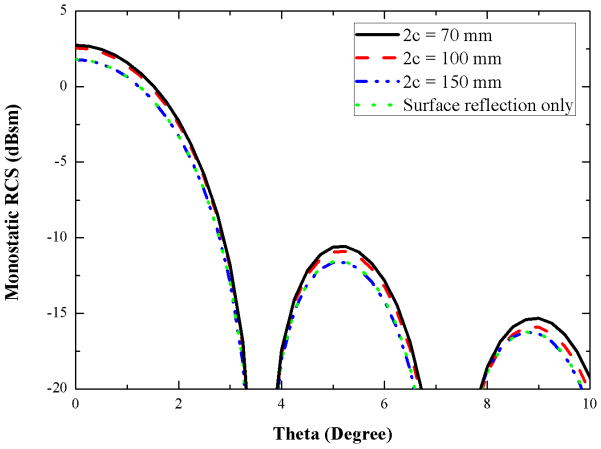

Figure 4. Monostatic RCS $\sigma_{\theta\theta}$ at 24 GHz from the top surface of the cuboids with different thickness $2c$. $a = b =$ 50 mm, $\varepsilon_r = 6.40 + i0.11$, $\phi = \phi_0 = 90^o$.

strong interaction yields the RCS oscillation for other directions. Then, the impact of the internal bouncing effect is demonstrated in Fig. 4. One observes that the bouncing effect is dependent on the cuboids's thickness. When the thickness is large, the bouncing effect is small and a good agreement can be seen with the result by only surface reflection. For thin bodies, the intense bouncing effect may vary the RCS value.

The effect of permittivity on the RCS values is shown in Fig. 5. As can be seen in (5) and (15), the monostatic RCS is dependent on the permittivity of dielectric objects. With high permittivity, the reflection coefficient is large. Then, the monostatic RCS increases. If the dielectric material has loss, namely the corresponding relative permittivity has a imaginary (negative) part, then the incident energy is attenuated in the transmission process inside the dielectric material. Therefore, when the imaginary part of the permittivity is larger, the internal bouncing effect is smaller.

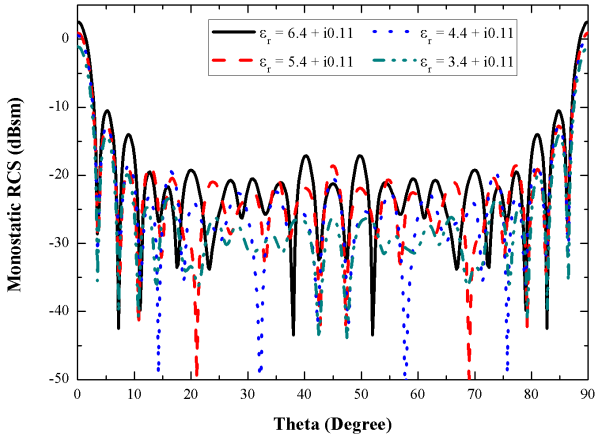

(a) With various real part of permittivity

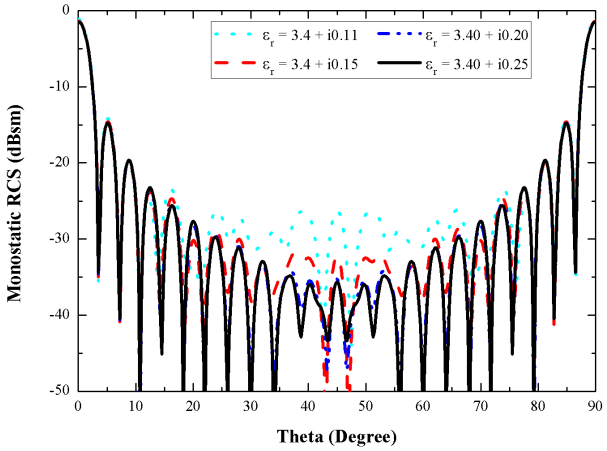

(b) With various imaginary part of permittivity

Figure 5. Monostatic RCS $\sigma_{\theta\theta}$ at 24 GHz form a cuboid with $a = b = c = 50$ mm.

The monostatic RCSs $\sigma_{\theta\theta}$ from the cuboids of the dimension 50 mm $\times$ 50 mm $\times$ 50 mm of Material 2 are calculated at 24 GHz and are compared with HFSS simulation results in Fig. 6. These numerical results are computed from the equivalent currents excited both at the top and the side surfaces of the cuboid. A symmetric monostatic RCS pattern with respect to angle $\theta = 45^o$ should be observed when the width $2b$ and the thickness $2c$ of the cuboid become the same. Our results show a good agreement with HFSS simulation results.

4 Conclusion

A formula to calculate the far field scattering from a cuboid illuminated by a TM polarized plane wave has been derived. The Kirchhoff approximation is applied to obtain the equivalent currents flowing on the surface, and the scattering fields are calculated by integrating the radiation field from these equivalent current sources. In this formula, the implementation of the collective reflection coefficient takes the multiple bouncing effect into account. The numerical calculated RCS values are compared with HFSS simulation results. The obtained result shows a good agreement with

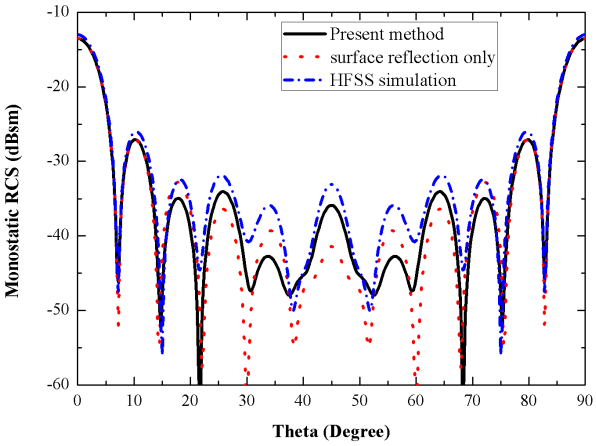

Figure 6. Monostatic RCS $\sigma_{\theta\theta}$ for a cuboid with $a = b = c = 25$ mm, $\varepsilon_r = 3.40 + i0.25$ and $\phi = \phi_0 = 90^{\circ}$ at 24 GHz.

HFSS simulation for monostatic RCS calculation.

Detail comparison for bistatic RCS as well as the polarization difference will be reported in the future.

References

[1] B. B. Baker and E. T. Copson, *The Mathematical Theory of Huygens Principle*, 2nd ed, London, Oxford University Press, 1950.

[2] T. Murasaki and M. Ando, "Equivalent edge currents by the modified edge representation: Physical optics components," *IEICE Trans. Electron.*, vol.E75–C, no.5, pp.617–626, May 1992.

[3] M. Oodo, T. Murasaki, and M. Ando, "Errors of physical optics in shadow region –Fictitious penetrating rays–," *IEICE Trans. Electron.*, vol.E77–C, no.6, pp.995–1004, June 1994.

[4] A. N. Nguyen and H. Shirai, "Electromagnetic wave scattering from dielectric bodies with equivalent current method," *Proc. of 2013 International Conference on Electromagnetics in Advanced Applications (ICEAA2013)*, pp. 744–747, 2013.

[5] A. N. Nguyen and H. Shirai, "Electromagnetic scattering analysis from rectangular dielectric cuboids –TE polarization–," *IEICE Trans. Electron.*, vol. E99–C, no. 1, pp. 11–17, 2016.

[6] M. Ishikawa and H. Shirai, "Non-contacting estimation of complex permittivity using RCS measurement," *Proc. of 2009 International Symposium on Antennas and Propagation (ISAP2009)*, pp. 588–591, 2009.